IDENTIFICATION OF NOISE SOURCES IN A HEATED JET FLOW

A Thesis

Presented in Partial Fulfillment of the Requirements for

Graduation with Distinction in the

Department of Mechanical Engineering at

The Ohio State University

By

Michael D. McDufford

*****

The Ohio State University
2006

Examination Committee:

Dr. M. Samimy, Adviser
Dr. J. Schmiedeler

Approved by

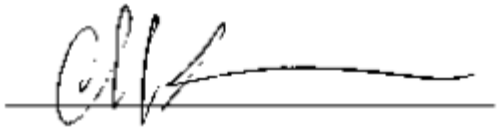

Dr. M. Samimy

Department of Mechanical Engineering

ABSTRACT

A heated jet facility has been recently designed and installed at the Gas Dynamics and Turbulence Laboratory (GDTL) at the Ohio State University. The purpose of this facility is to simulate the exhaust flow conditions from both a commercial aircraft (jet exhaust Mach number of 0.9) and an advanced military aircraft (jet exhaust Mach number of 2.0). Previously, the GDTL used, with great success, an ideally expanded Mach 1.3 cold jet since this jet's exhaust velocity was close to an actual commercial jet engine exhaust. The exhaust of a commercial jet engine, though, is heated due to the combustion process that takes place in the combustor of the engine. Since a Mach 0.9 heated jet flow is typical of commercial engines, this new heated jet facility will provide a more accurate model of an actual jet engine's exhaust, which will be the focus of this proposed research.

The GDTL put a major effort in recent years in designing flow, acoustic, and mathematical tools to identify noise sources in a Mach 1.3 cold jet. The main goal of this research is to use some of these tools to obtain detailed jet noise source data in a Mach 0.9 heated jet. This data will be used to gain preliminary understanding of the differences between the noise generated in a heated flow and the noise generated in a cold flow to help develop ways to mitigate this noise. This thesis will focus on the steps taken thus far to ensure that this new heated jet facility is operating as expected and providing "clean" noise data. Some preliminary analysis of heated jet noise spectra, up to 600 ^{o}F at angles of 30^{o} and 90^{o} to the jet axis, and the subsequent results and conclusions will also be discussed including issues encountered with the lowering of the jet's Reynolds number with heating.

ACKNOWLEDGEMENTS

First off, I would like to thank my adviser, Dr. Mo Samimy, for giving me the chance to conduct undergraduate research and for his guidance and support all along the way. I would also like to give a big thanks to Jeff Kastner for always helping me with the day to day running of experiments and data analysis and for being able to always answer the countless questions I had along way. I would lastly like to thank the rest of the GDTL staff for all of their support and for creating a friendly and fun lab environment.

TABLE OF CONTENTS

LIST OF FIGURES AND TABLES

Figures **Page**

Tables

CHAPTER 1

INTRODUCTION

Jet noise has become an important issue today because the current levels of noise produced by jet engines are still above acceptable limits, particularly during takeoff. This leads to unacceptable noise pollution and consequently places a financial burden on an already struggling commercial aerospace industry. This is because some airports have flight restrictions during certain hours based on noise generated and a reduced number of flights must be flown. Also, if the noise level of aircraft engines is above a certain level, airports can be financially penalized. The development of high-bypass ratio turbofan engines has helped to alleviate jet noise somewhat by reducing the effective velocity of the jet exhaust. Further reductions in jet noise are still needed, though, and the large bypass ratios of modern commercial engines are reaching their limits (Hileman 2004). Thus, new methods of jet noise reduction need to be developed and implemented.

In order to enhance the development of new jet noise reduction techniques, an accurate model of jet exhaust needs to be developed and a better understanding of the physical mechanisms in a jet flow that generate noise needs to be gained. In recent research efforts at the GDTL jet facility, a Mach 1.3 cold jet has been used to model the exhaust of a commercial jet engine. A Mach 1.3 cold jet was chosen because it has the same convective velocity as a typical commercial jet engine exhaust, which is around Mach 0.9 with a stagnation temperature of 810 K (1000 ^{o}F) (Southworth). By using a 3-D microphone array and a laser-based flow visualization system, researchers at the GDTL were able to qualitatively correlate the interactions of large-scale structures in the

jet's shear layer during periods of noise generation and relative quiet to the far field noise (Hileman et al. 2004). From these experiments, it was determined that one of the main mechanisms behind jet noise was the interaction of these large-scale turbulence structures as they "tilt, stretch, tear, and pair" with each other (Hileman et. al 2002b). These results were for an ideally expanded Mach 1.3 cold jet and while this jet is a good approximation of commercial jet engine exhaust, it is certainly not the best model since it fails to include the effects of temperature on jet noise. Due to the combustion process in the engine, jet engine exhaust is very hot and this elevated temperature leads to additional sources of noise in the jet that would not be captured by only studying cold flow (Mani 1976).

Thus, in order to develop a more accurate model of jet noise, a new heated jet facility was implemented at the GDTL that will allow for controlled heating of a jet flow. Much of this thesis will detail the implementation of this new facility, most notably the heater, and the obstacles that had to be overcome (and in some cases, obstacles that are still being overcome). A large part of the thesis (most of Chapter 3) will deal with the implementation of the electric storage heater at the GDTL chosen to provide heat to the flow and the subsequent barriers that have had to be overcome to provide predictable and quiet heating. In Chapter 4 of this thesis, the first round of Mach 0.9 heated jet data acquired with the new heated jet facility will be presented in order to show the high quality of data the new facility provides and to show the basic effects of temperature on the sound pressure level (SPL) of a jet flow.

Based on the SPL results that were taken from the heated Mach 0.9 jet, the effects of temperature on the jet Reynolds number and exit boundary layer conditions will be discussed. It will be shown that potential Reynolds number effects exist in the jet flow at

elevated temperatures and that boundary layer tripping is needed in the GDTL facility. Chapter 4 will conclude with a discussion of the design process for a tripping mechanism that has been manufactured for the GDTL jet facility. Finally, an overall summary of the results of this research effort, as well as recommendations for future work, will be presented in Chapter 5.

CHAPTER 2

BACKGROUND

Section 2.1 – Jet Noise Theory

The development of jet noise theory began in 1952 when Lighthill linked the intensity of jet noise to the nth-power of the relative jet exhaust velocity. It was later determined that for lower Mach number jets, the noise intensity is proportional to the 8^{th} power of the relative jet velocity and for higher Mach number jets the noise intensity is proportional to the 3^{rd} power of the relative jet exhaust velocity (Lilley 1991). Lighthill's approach was strictly mathematical, though, and his governing equation did not lend insight into the specific physical mechanisms that govern jet noise.

Through various research efforts over the years, it has been determined that jet noise is physically caused by the interaction of turbulence structures in the jet's shear layer. A general schematic of the different regions of jet exhaust is shown in Figure 2.1. The jet's shear layer, referred to as the mixing region of the jet in Figure 2.1, is the boundary between the exhausting jet flow and the ambient air. In this shear layer, the turbulence structures (referred to as "eddies" in Figure 2.1) are formed from the shearing between the high-speed jet flow and the ambient air. These turbulence structures have different length scales associated with them. The fine-scale turbulence structures ("small eddies" in Figure 2.1) are formed near the jet exit and radiate noise in directions close to perpendicular with the jet axis (Tam et. al 1996). The large-scale turbulence structures ("large eddies" in Figure 2.1) are formed further downstream of the nozzle exit as the shear layer grows and the smaller-scale turbulence structures begin to interact and

combine. The large-scale turbulence structures tend to radiate noise in the downstream direction as they travel downstream (Tam et. al 1996, Hileman 2004). The cone shaped area close to the nozzle exit and before the mixing layer is known as the potential core of the jet and is the region where the jet flow is still uniform and no mixing is taking place.

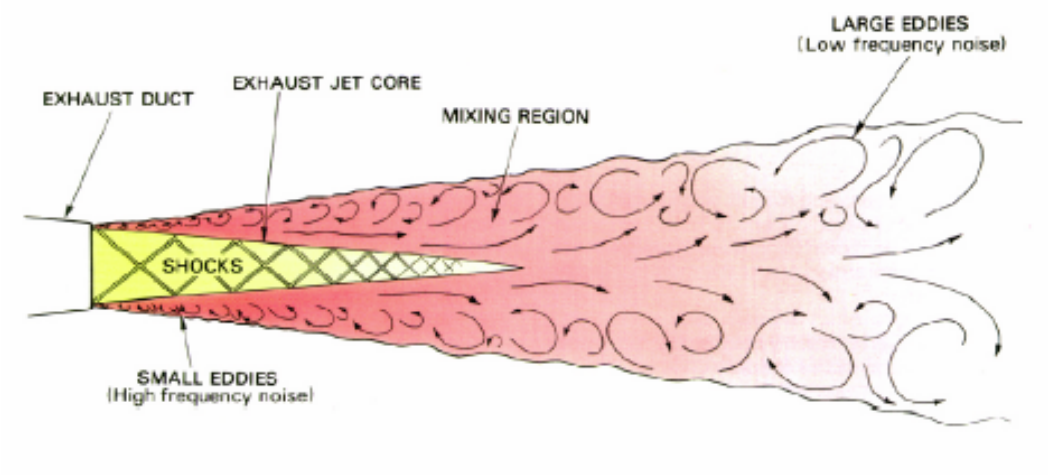

Figure 2.1 – Schematic showing the different regions of an exhausting jet flow (Antoine 2000).

Since different turbulence structure scales radiate noise in different directions, the SPL observed from the jet will be different depending upon the angular location relative to the jet axis. Figure 2.2 shows how the jet noise spectra changes for an observer at an angle, θ, from the jet axis. As θ is increased, the SPL peak levels are over a narrower frequency band and peak amplitude increases with the maximum SPL observed at $\theta = 30^{o}$. The lowest SPL peak amplitude is observed at $\theta = 90^{o}$. It is important to note that θ will always be measured from the jet axis as shown in Figure 2.2 in this paper.

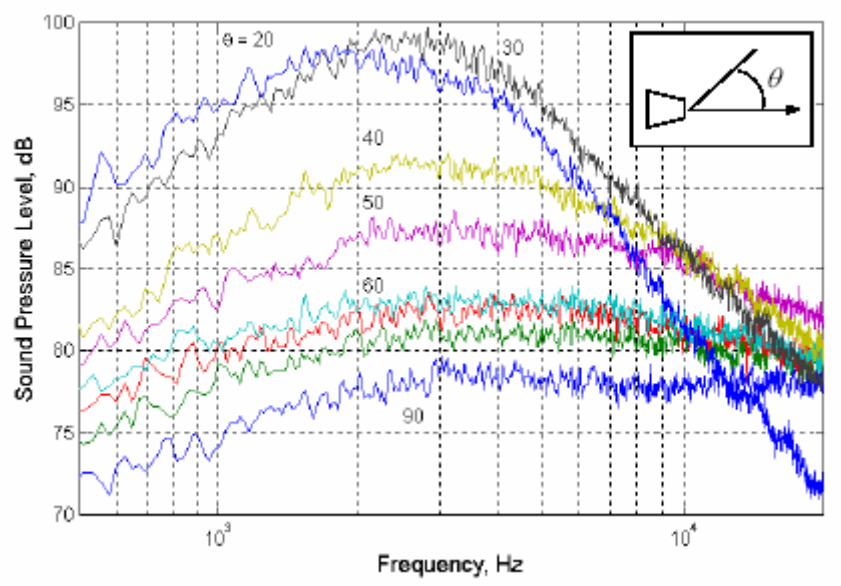

Figure 2.2 – The effect of changing observation angle on the observed far-field acoustic spectra of a jet. In this paper, SPL data will be taken at θ = 30° and θ = 90 ° as defined in this figure (Hileman 2004).

Since the overall goal of studying jet noise is to reduce it and the loudest jet noise is heard at $\theta = 30^{o}$, a lot of jet noise data is taken from 30^{o} to try to understand the specific mechanisms that are responsible for the noise in this direction. Recently at the GDTL, a 3-D eight microphone array oriented at $\theta = 30^{o}$ was used to determine the locations where noise is generated in a Mach 1.3 cold jet flow. In conjunction with the 3-D microphone array, a laser-based flow visualization system was used to capture images of the Mach 1.3 jet. By correlating the data from the 3-D microphone array and the flow visualization system, the interactions and physical characteristics of the large-scale turbulence structures during periods of noise generation were captured. From these experiments it was shown that the loudest noise peaks were produced in the jet when the large-scale turbulence structures interact near the end of the potential core, roll up into each other, tear and stretch (Hileman 2004). This was the first time that the specific

interactions of the large-scale turbulence structures in the jet mixing layer were visualized during actual periods of noise generation and tremendous insight was gained as to the physical mechanisms in a jet that cause noise. Still the data was mostly qualitative in nature and much work still needs to be done.

2.2 – Heated Jet Noise – The Effects of Increased Temperature

Due to the success at the GDTL in observing the physical structures that are responsible for the loudest jet noise in Mach 1.3 cold jets, the interest has turned to studying heated jets. Since an actual jet engine's exhaust is heated to around 1000 ^{o}F, a Mach 0.9 heated jet provides a better model for a jet engine exhaust flow since the temperature effects on the jet noise can be captured.

To begin to understand the effects of temperature on jet flow it is necessary to first define a few terms and equations. First off, the jet Mach number, M, is the ratio of the jet velocity, V_j, at the nozzle exit to the local speed of sound in the jet flow, a, and is given by the following equation:

$$M = \frac{V_j}{a} \quad (1)$$

$$\text{where, } a = \sqrt{\gamma RT} \quad (2)$$

In equation (2), γ is the ratio of specific heats and is equal to 1.4. R is the gas constant and is equal to 287 J / (kg-K). T is the static exit temperature of the jet in absolute units. For the current study the jet was run only at Mach 0.9. Substituting equation (2) into (1) and solving for V_j yields:

$$V_j = M\sqrt{\gamma RT} \quad (3)$$

From equation (3), it follows that for a constant Mach number, V_j will increase in proportion to $T^{1/2}$. Since jet noise is proportional to the 8th-power of V_j it seems that the jet noise will increase as temperature increases (again, assuming a constant Mach number).

Temperature also impacts the Reynold's number of the jet. The Reynold's number is a non-dimensional parameter that partially characterizes the amount of turbulence in a jet flow and whether the boundary layer of the flow is turbulent, transitional or laminar. It is given by the following equation:

$$\mathrm{Re} = \frac{\rho D_j V_j}{\mu} = \frac{D_j V_j}{\nu} \qquad (4)$$

In equation (4), D_j is the diameter of the jet nozzle and is always 1 inch, ρ is the jet flow density, μ is the jet dynamic viscosity and ν is the kinematic viscosity. In general, as the Reynold's number of the jet increases the turbulence in the jet increases. As shown before, V_j increases with increasing temperature, which would thus increase the Reynold's number. However, the kinematic viscosity also increases with increasing temperature and more rapidly than V_j. Thus, as temperature is increased the Reynold's number of the jet decreases. As the Reynold's number of the jet decreases, the turbulence in the jet decreases and if the Reynold's number decreases far enough, it is possible for the jet's boundary layer to change from turbulent to transitional or laminar. This is known as the "Reynold's number effect."

If the jet boundary layer transitions away from turbulent, the physical structure of the jet will change and different mechanisms will become responsible for jet noise. This

situation is undesirable and if it occurs a way must be devised to enhance the turbulence of the flow and restore the validity of the jet model.

CHAPTER 3

EXPERIMENTAL SETUP

3.1 – Mach 0.9 Nozzle Design

All the data obtained in this research effort and presented and discussed in Chapter 5 was obtained using an axis-symmetric Mach 0.9 converging nozzle with an exit diameter of 1 inch. A picture of this nozzle is shown in Figure 3.1. The nozzle was made of stainless steel in order to withstand temperatures in excess of 1000 ^{o}F. In order to ensure an ideally expanded flow, the inner contour of the nozzle had to be designed such that there were no abrupt area changes or discontinuities in the contour. If discontinuities were present in the contour, the jet noise spectra would likely contain unwanted SPL peaks. Also, discontinuities would cause losses in the flow and the desired exit Mach number of 0.9 would not be reached since the pressure ratio used to obtain a Mach 0.9 flow assumes an isentropic expansion.

Figure 3.1 – Picture of the Mach 0.9 converging nozzle used to obtain all the data shown in this thesis. The nozzle is made of stainless steel and has an exit diameter of 1 inch.

The nozzle inner contour was generated using a MATLAB script. In the script, a 3rd-order polynomial is fitted between the nozzle inlet point and the nozzle exit point. This 3rd-order curvature is then approximated using two circles and a line to get the final curvature. An error-minimizing algorithm was put in the script to ensure that the chosen circle radii and line slope formed a contour that almost perfectly matched the baseline 3rd-order polynomial. Approximating the baseline polynomial curve in this fashion greatly eased the machining process since the machinist only had to worry about matching two radii and a line, rather than points along a polynomial curve. It is important to note that past experience at the GDTL has shown this method of converging nozzle design yields nozzles that produce clean noise spectra.

3.2 – GDTL Heated Jet Facility

All the experiments run for this research effort were conducted at the GDTL jet facility located at the Ohio State University's Don Scott Airport. The GDTL facility uses microphone arrays and a laser-based flow visualization system to study the mechanisms of noise generation in jets of various Mach numbers when fully setup. For this specific research effort, only microphones located at 30^o and 90^o to the jet axis were needed. No flow-visualization needed to be performed either. The facility is designed so that it can handle 1 inch exit diameter nozzles designed for a wide range of subsonic and supersonic Mach numbers. A schematic of the setup used for the experiments in this effort is shown in Figure 3.2.

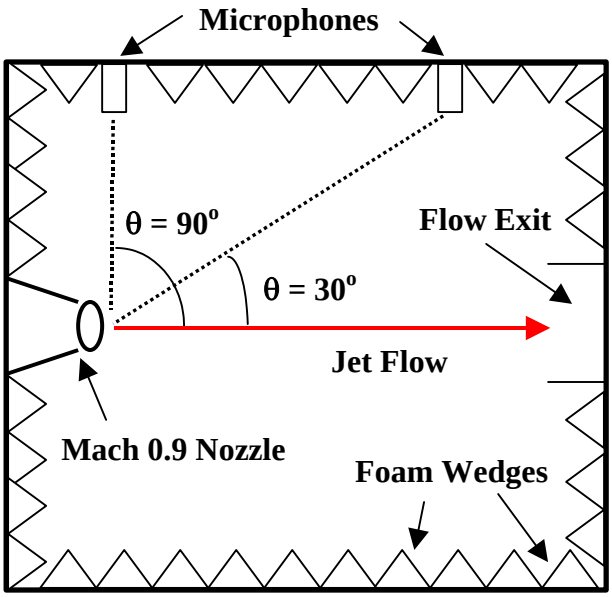

Figure 3.2 – Schematic of the GDTL jet facility setup used to collect the jet noise results.

The air supply for the jet facility is supplied by two tanks located outside of the facility. The air is stored at 16.5 MPa and the capacity of the two tanks together is 42.5 m^3. These tanks also serve other experimental facilities at the GDTL, so a control valve system has been setup that controls which facility the air goes to. The overall valve system is controlled from a control panel located in the middle of the lab area. As the air flows from the supply tanks to the jet facility, the valve system also reduces the air pressure to the required amount. A control panel located near the jet facility provides the automatic control interface used to set and maintain the required jet stagnation pressure for the desired jet Mach number. The panel also displays the stagnation temperature of the jet. This control panel is shown in Figure 3.3.

Figure 3.3 – The control panel used to control the GDTL jet facility. The control system allows for automatic control of the jet stagnation pressure in order to provide a constant Mach # flow.

After passing through the valve system, the air flows through the jet facility stagnation chamber where it passes through a set of flow screens and gets straightened and conditioned. A side view of the jet stagnation chamber is shown in Figure 3.4. The length of the chamber is such that extraneous flow noise is eliminated before the flow reaches the exit of the chamber. From the stagnation chamber, the air flows through a set of extensions and then passes through the jet nozzle and is accelerated to the appropriate Mach number. The jet flow then exits through the nozzle into an anechoic chamber where the microphones are located. Foam wedges in the anechoic chamber absorb sound waves and minimize sound wave reflections that would contaminate the SPL data collected by the microphones. The chamber is almost completely sealed in order to block

outside noise from contaminating the data. There are openings in the chamber in the corners on the nozzle side since the jet has to have an ample supply of ambient air to entrain while it flows downstream in the chamber. The jet exits the chamber through a large bell-mouth plenum opposite of the nozzle exit.

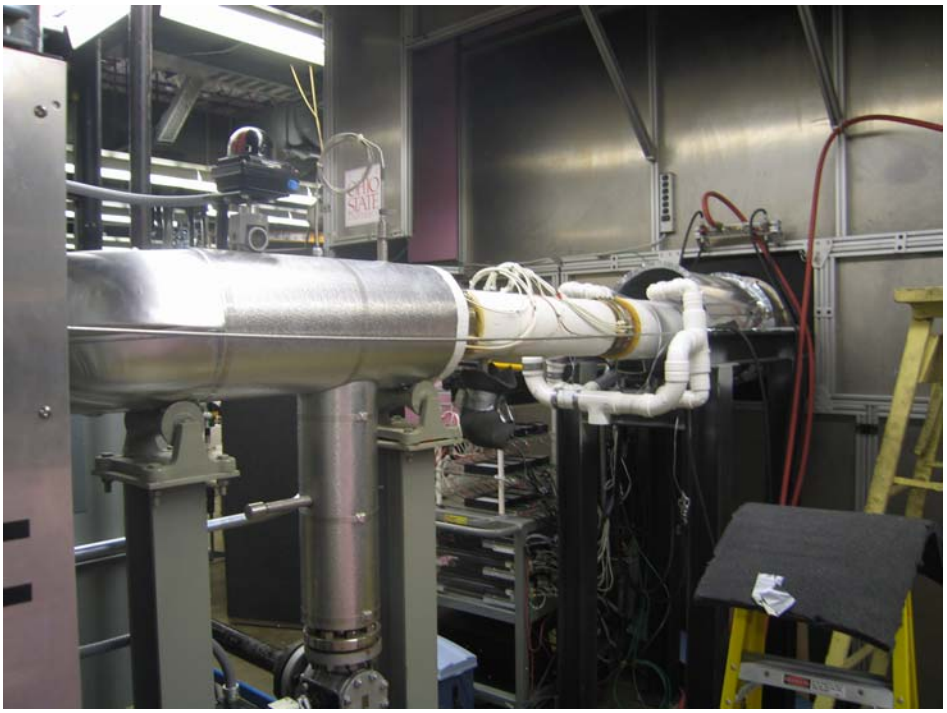

Figure 3.4 – A side view of the jet stagnation chamber. The air enters from the heater on the left and flows to the right and into the anechoic chamber.

While flowing through the anechoic chamber, the noise generated by the jet is measured by various microphones hung at different locations throughout the facility. For this experiment, microphones at 30^o and 90^o to the jet axis (using the angular reference shown in Figure 2.2) were used but the facility allows for a microphone at 60^o as well as other various microphone configurations and arrays. The microphones used in these experiments are Bruel and Kajer ¼ inch condenser microphones. Prior to each

experiment, each microphone was calibrated with a Bruel and Kajer calibrator that gives a 94 dB signal at 1 kHz. Since the microphones have a flat frequency response over the frequencies of interest, they only needed to be calibrated at one point in that range. The microphone signals pass through a Bruel and Kajer Nexus conditioning amplifier and band-pass filter from 100 Hz to 100 kHz. Finally, the microphone signals are picked up by a PC-6110E data acquisition board and collected by a computer using Labview software.

3.3 – Heating the Flow – The Jet Facility Heater

The new GDTL heated jet facility uses a large electric storage heater, shown in Figure 3.5, to provide heating to the jet flow. An electric storage heater was chosen because it provides quiet heating and will not add noise to the flow, unlike a loud combustion process. The heater works by using a small motor that pulls in air into the heater system. This air is passed through the main electric heating unit where the air is heated up to a very high temperature. The air then flows into the large storage chamber where it passes over and heats up densely stacked steel plates. The heater's piping system is controlled by a set of manual valves that can be open and closed to direct the heated flow as desired. While heating, the heater is a self-contained unit from the jet facility and all the heated air flow exhausts to the outside after dumping its energy into the storage chamber. When it is time to run heated jet experiments, the valve positions are altered appropriately and the air from the outside storage tanks is directed through the steel plates in the heater's storage chamber and gets heated up before being directed back

to the jet facility. The heater is operated using a control panel attached to the side of it where users can input the desired temperature for the storage chamber.

Figure 3.5 – (Left) The storage heater used to provide heat to the jet facility. (Right) The other side of the storage heater showing the jet facility control panel from Figure 3.3 (the heater is undergoing modification in both of the pictures here).

According to specifications, the heater is designed to handle up to Mach 2.0 flows and temperatures over 1000 ^{o}F. The heater should also be able to reach these high temperatures in around 8 hours or so, the goal being to turn the heater on early in the morning and run experiments later in the day. Unfortunately, the heater has not been able to reach these specifications. Although it has provided very clean and quiet flow, the heater has only been able to reach a maximum temperature of around 600 ^{o}F with well over 12 hours of heating on different days. Also, the heater only came with two

thermocouples: one placed in the electric heating unit (input temperature) and the other placed at the bottom of the storage tank where the jet flow exits the heater before passing into the jet facility (output temperature). The thermocouple readings are output to the heater control panel. As will be shown, though, neither of these thermocouple readings seem to match the final jet stagnation temperature.

The first test of the heater was performed using the Mach 0.9 nozzle discussed previously. A plot of the heater output temperature vs. heating time is shown in Figure 3.6. Even after 10 hours of heating on the first day, the heater output temperature only reached 300 ^{o}F and from the plot, showed signs of slowing down.

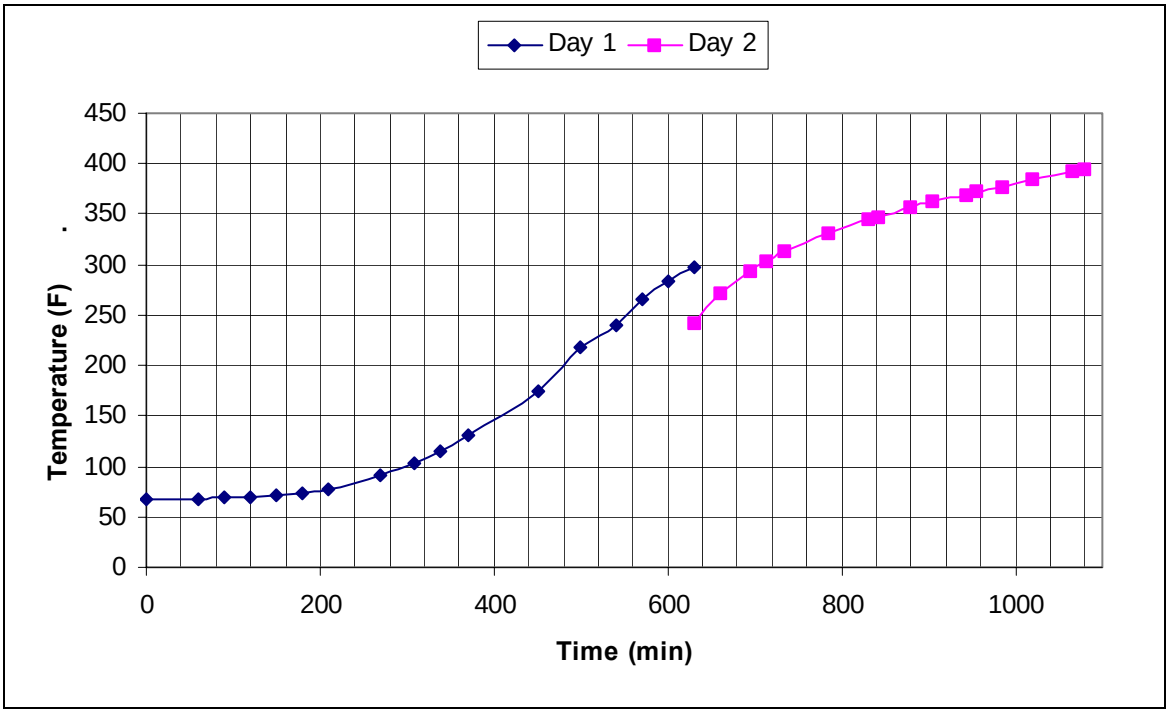

Figure 3.6 – Plot of the heater output temperature vs. heating time during the first heating test run.

The heater was allowed to cool overnight in order to let the heat in the storage tank diffuse more evenly. From simply touching the tank, it was apparent that only the top of the storage tank where the flow enters was getting hot and that the heat was not spreading to the plates in the bottom of the storage tank. The next day, the heater was run for around 6 more hours and only reached an output temperature of 400 ^{o}F, which is far short of the specifications.

The decision was made to run at this point, though, in order to see what jet stagnation temperature would be produced and to see how long the jet would remain at this temperature. Figure 3.7 shows the results of this first run. The jet stagnation temperature ended up being 424 ^{o}F, which was somewhat close to the heater output temperature of 400 ^{o}F, but still unacceptably off. The absolute stagnation temperature of the jet, however, was kept for around 30 minutes within 1%, which was acceptable.

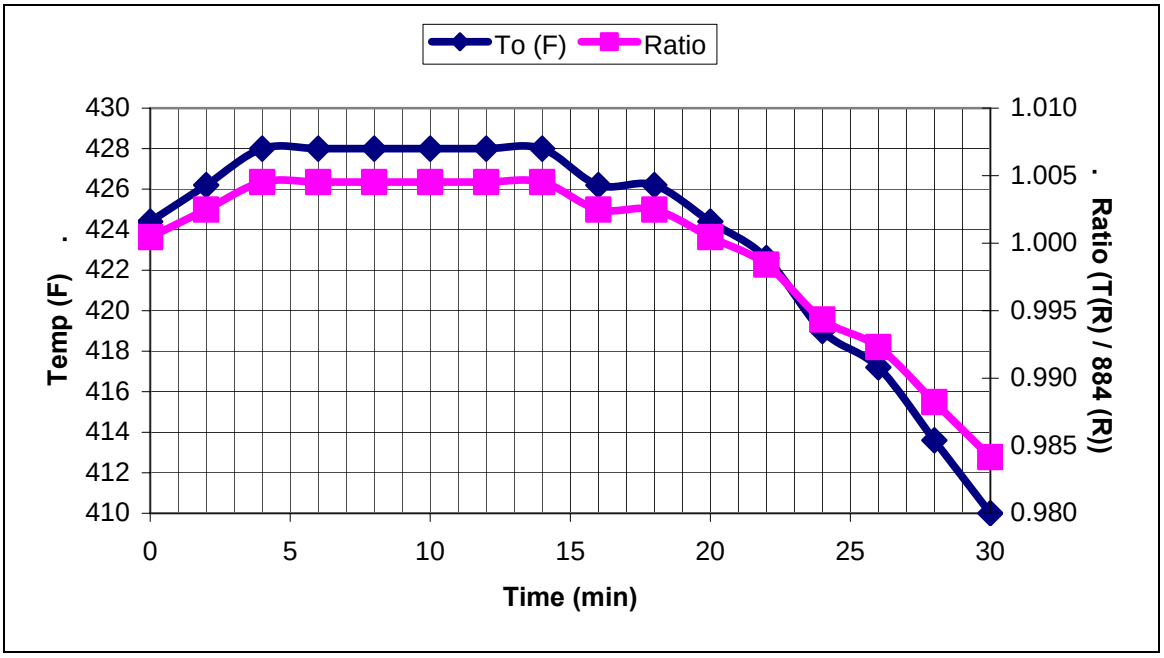

Figure 3.7 – Plot of the jet stagnation temperature vs. operating time during the first heated jet run.

From this first round of experiments with the heater it was concluded that the heater did not have enough insulation and that the heat in the storage tank was escaping before reaching the bottom of the storage tank. Thus, the company responsible for the heater agreed to put more insulation around the storage tank and also the heater system piping. Another round of experiments was run with the new insulation and unfortunately the situation did not improve much. The heater was able to achieve a jet stagnation temperature of 600 ^{o}F but nothing higher and it took two days of heating to get there. Also, the heater output thermocouple showed an output temperature of 428 ^{o}F, once again showing that the heater was not predictable based on the current thermocouple locations. Since time was getting a bit short, it was decided to take heated jet data up to a stagnation temperature of 600 ^{o}F for this research effort since further modifications to the heater would take several weeks.

Despite lacking the desired heating capacity, the heater performed very well from a noise standpoint. The motor on the heater ran very quietly and no noise from the heater seemed to enter the anechoic chamber and get picked up by the microphones. In Figure 3.8 a Mach 0.9 jet spectrum taken with the new storage heater is shown. The sound spectrum is smooth throughout and no high-SPL tones or anything unexpected is seen. Also in Figure 3.8, a contaminated noise spectrum that was obtained during a previous attempt to implement flow heating at the GDTL is shown. As can be seen this older heater produced high-decibel tones in the jet spectrum leading to unacceptable data contamination.

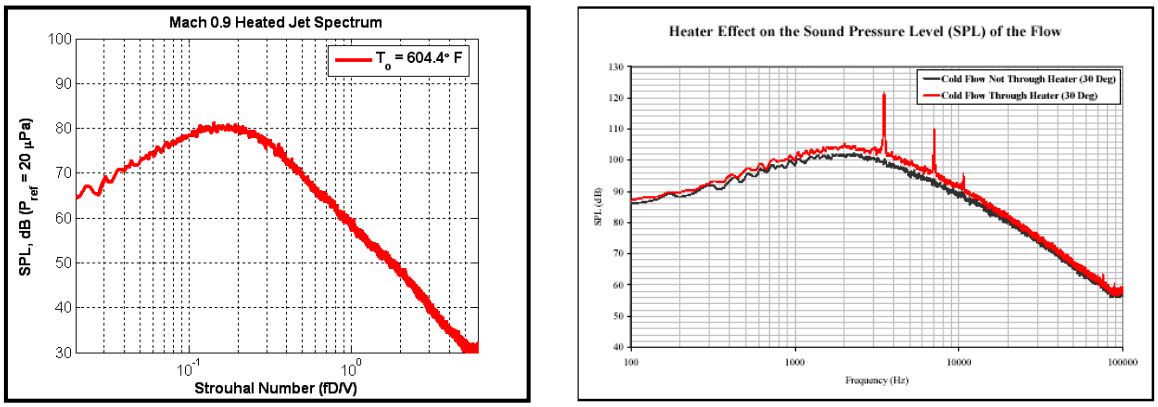

Figure 3.8 – (Left) Mach 0.9 heated spectrum using the new heater. (Right) Jet noise spectrum obtained using the old heater (Southworth 2004).

At the time of writing, the heater is currently being rebuilt with several modifications. These modifications include a larger motor to increase the mass flow rate of air through the heater in order to push hotter air into the bottom of the storage tank. Also, external band heaters are being put around the storage tank to aid in heating and more thermocouples placed in more useful places are being installed, along with an entire new control panel. It is expected that these changes will increase the heater output temperature, produce a predictable jet stagnation temperature and greatly decrease the required heating time.

3.4 – Definitions of Experimental Parameters and Ambient Conditions

As stated before, all heated jet spectra were obtained using the Mach 0.9 converging nozzle discussed in section 3.1. Due to the problems with the heater outlined in section 3.3, the heated jet spectrums were obtained up to a jet stagnation temperature of 600 ^{o}F, rather than 1000 ^{o}F as originally desired. Spectra were collected at temperatures of 50 ^{o}F and then from 600 ^{o}F down to 200 ^{o}F in increments of 50 ^{o}F. The

50 ^{o}F jet will be referred to as the cold jet. The lower heated temperatures were obtained by simply letting the jet run from one temperature point until it cooled down to the next desired temperature. In order to speed the cooling up, the jet Mach number was usually increased to provide a greater mass flow rate and pull energy out of the storage tank quicker. It was of course turned back down to Mach 0.9 before sound data was acquired.

The ambient pressure on the day of experimenting was 975.5 mbar or 14.15 psi. For a Mach 0.9 jet, the ratio of stagnation pressure to static pressure is 1.691 leading to a required stagnation pressure of 23.93 psig (Anderson). This stagnation pressure was maintained throughout the experiment through the automatic pressure control system installed at the GDTL and discussed in section 3.3.

As outlined in section 3.3 also, microphones at 30^{o} and 90^{o} to the jet axis were used to capture the sound pressure data. The 90^{o} microphone was located 44 inches from the nozzle exit and the 30^{o} microphone was located at 83 inches from the nozzle exit. These distances will become important in Chapter 4 when the jet sound gets scaled. The microphone data was acquired by the data acquisition system at a sampling rate of 200 kHz. 100 blocks of data were taken for each spectrum with each block consisting of 8192 points. This yielded a frequency resolution of 24.41 Hz for the jet noise spectrums.

CHAPTER 4

RESULTS

4.1 – Heated Jet Spectrums at 30^o and 90^o.

The following graphs show the SPL of the heated jet between 50 ^{o}F and 600 ^{o}F. Two microphone locations at 30^o and 90^o were used to obtain this sound data. For each microphone location, three graphs will be shown. The first graph for each location will show the SPL obtained for each temperature plotted versus frequency. This will be considered the raw data set since no scaling has been applied. The second graph for each location will show the SPL for each graph plotted against Strouhal number. This serves to non-dimensionalize the frequencies of each heated jet and allows for a better comparison of each one. Also, scaling by the Strouhal number allows for better facility-to-facility comparison. The Strouhal number is given by equation (5):

$$S_{td} = \frac{fD_j}{V_j} \quad (5)$$

In equation (5), f is the frequency of interest in Hz.

In the third and final graphs the SPL of each jet will be scaled by the jet velocity, which will increase as the temperature of the jet increases. In this third graph, the spectra are also normalized to a microphone distance of 80 inches and atmospheric absorption effects are also taken into account per ANSI SI.26. For the atmospheric absorption effects, a standard day temperature of 298 K and a relative humidity of 50% were used. The final scaling equations for 30^o and 90^o are given below:

For 30°: $$SPL_{corr} = SPL - 80\log_{10}(\frac{V_j}{V_{j,cold}}) + 20\log_{10}(\frac{r}{80}) + A_{corr} \quad (6)$$

For 90°: $$SPL_{corr} = SPL - 42\log_{10}(\frac{V_j}{V_{j,cold}}) + 20\log_{10}(\frac{r}{80}) + A_{corr} \quad (7)$$

The first term on the left-hand side in equations (5) and (6) is the baseline SPL of the jet at each temperature before any correction. The second term is the velocity correction and the third term is the microphone distance correction with the microphones normalized to a distance of 80 inches. For the 30° microphone, r is 83 inches and for the 90° microphone, r is 44 inches. The fourth and final term, A_{corr}, is the correction for atmospheric absorption effects.

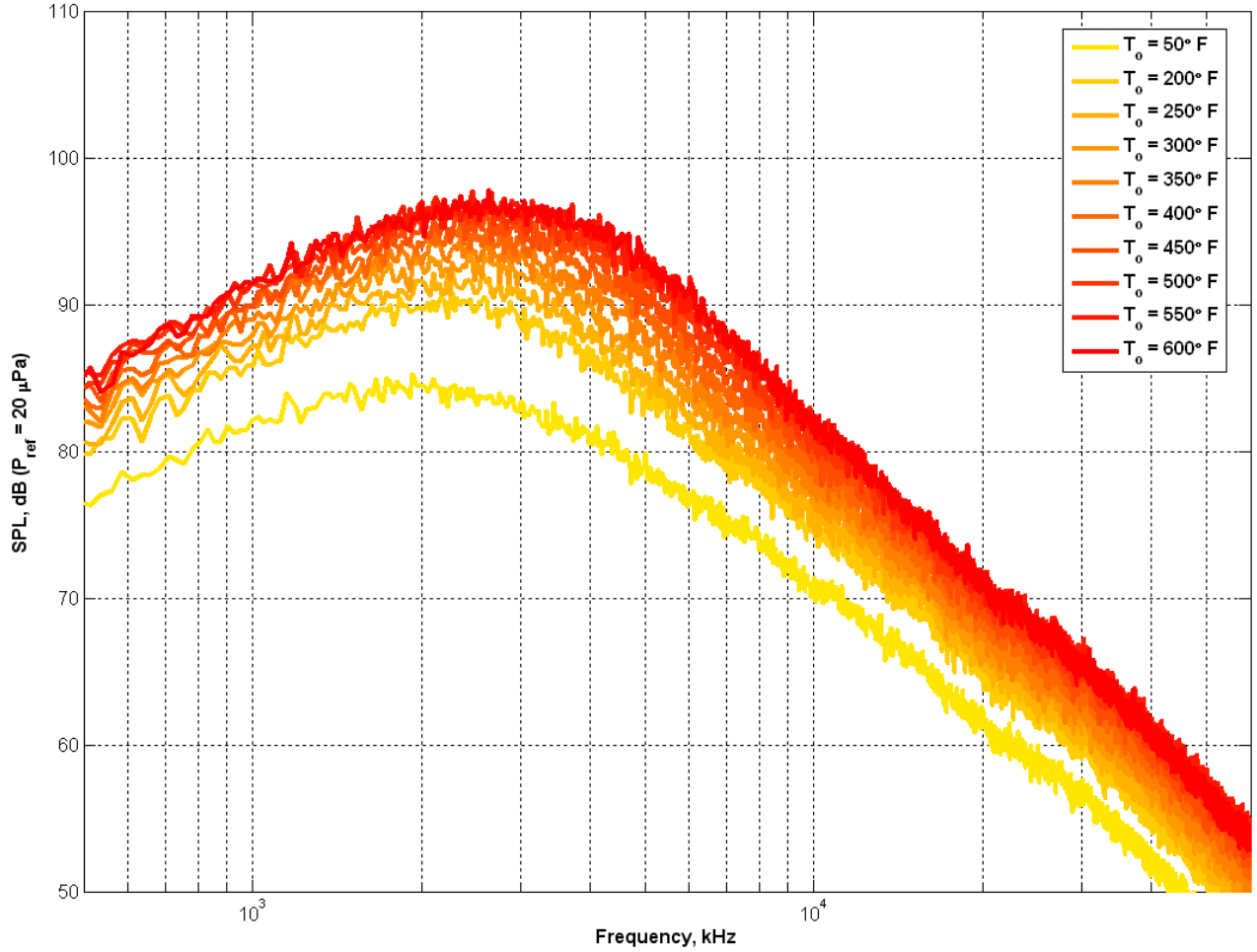

Figure 4.1 – Mach 0.9 heated jet spectra taken at $\theta = 30^0$. These are the raw data sets before any scaling has been applied.

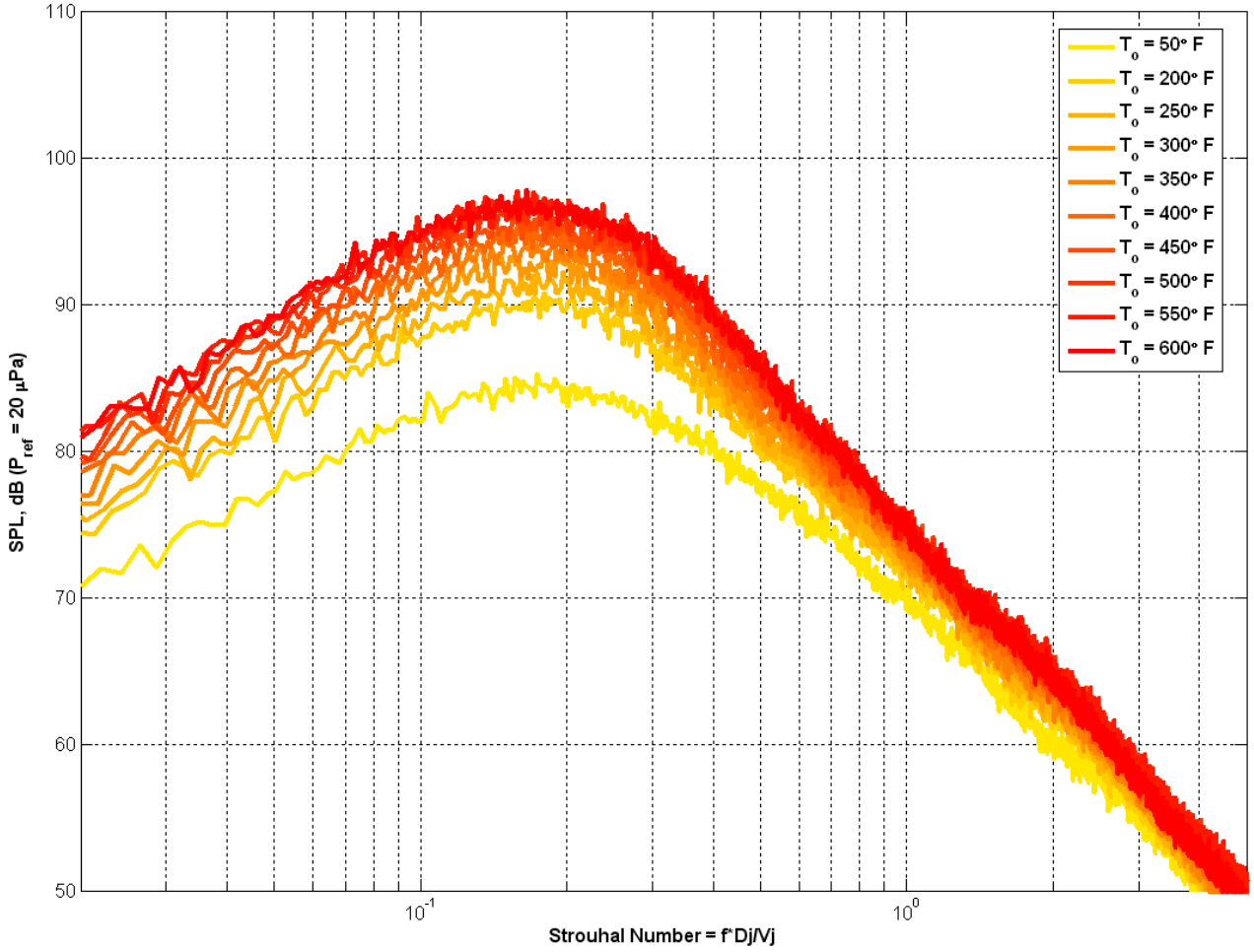

Figure 4.2 – Mach 0.9 heated jet spectra taken at $\theta = 30^0$. Frequency has been normalized by the Strouhal number.

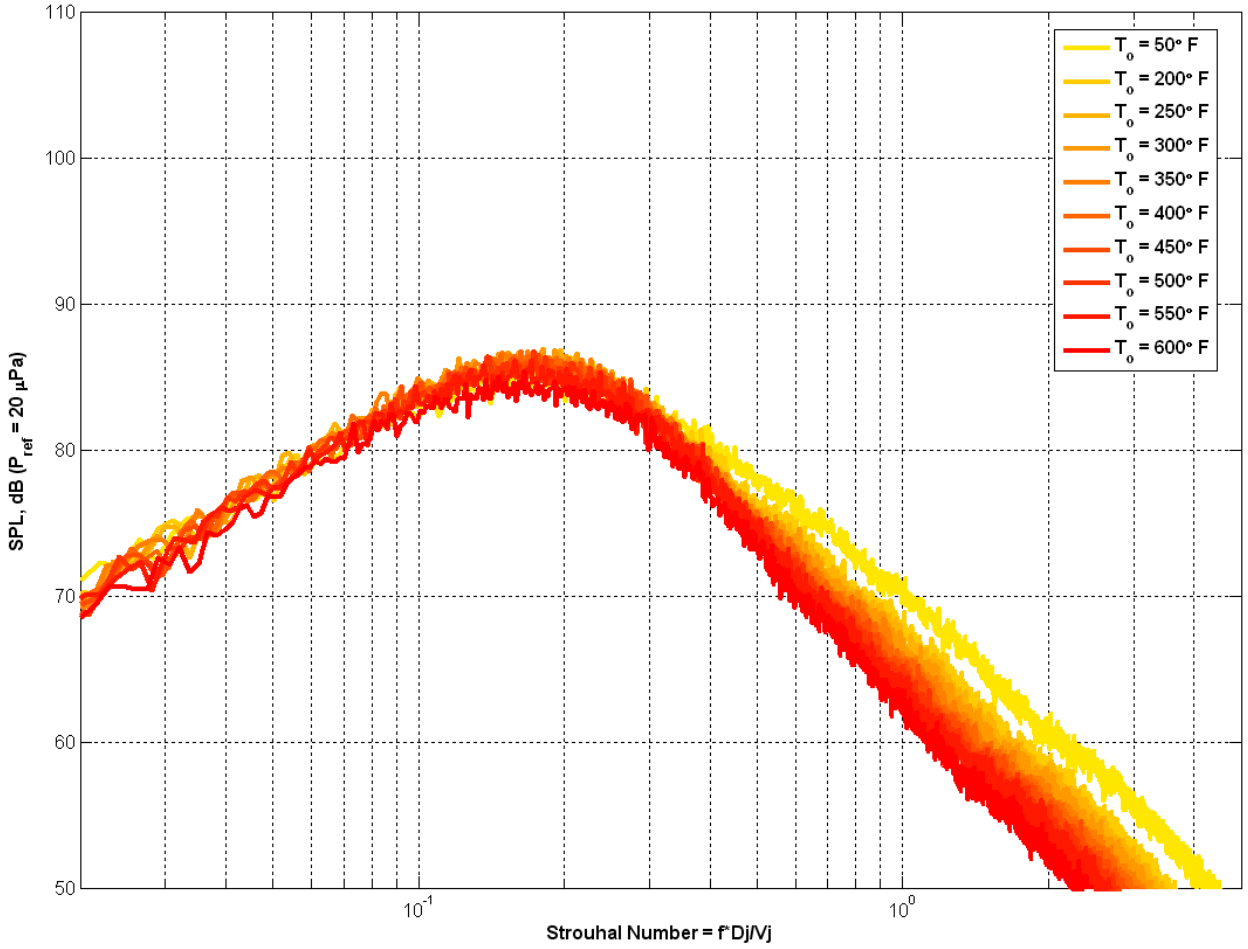

Figure 4.3 – Mach 0.9 heated jet spectra taken at $\theta = 30^0$. Frequency has been normalized by the Strouhal number and the SPL for each temperature has been normalized using equation (6).

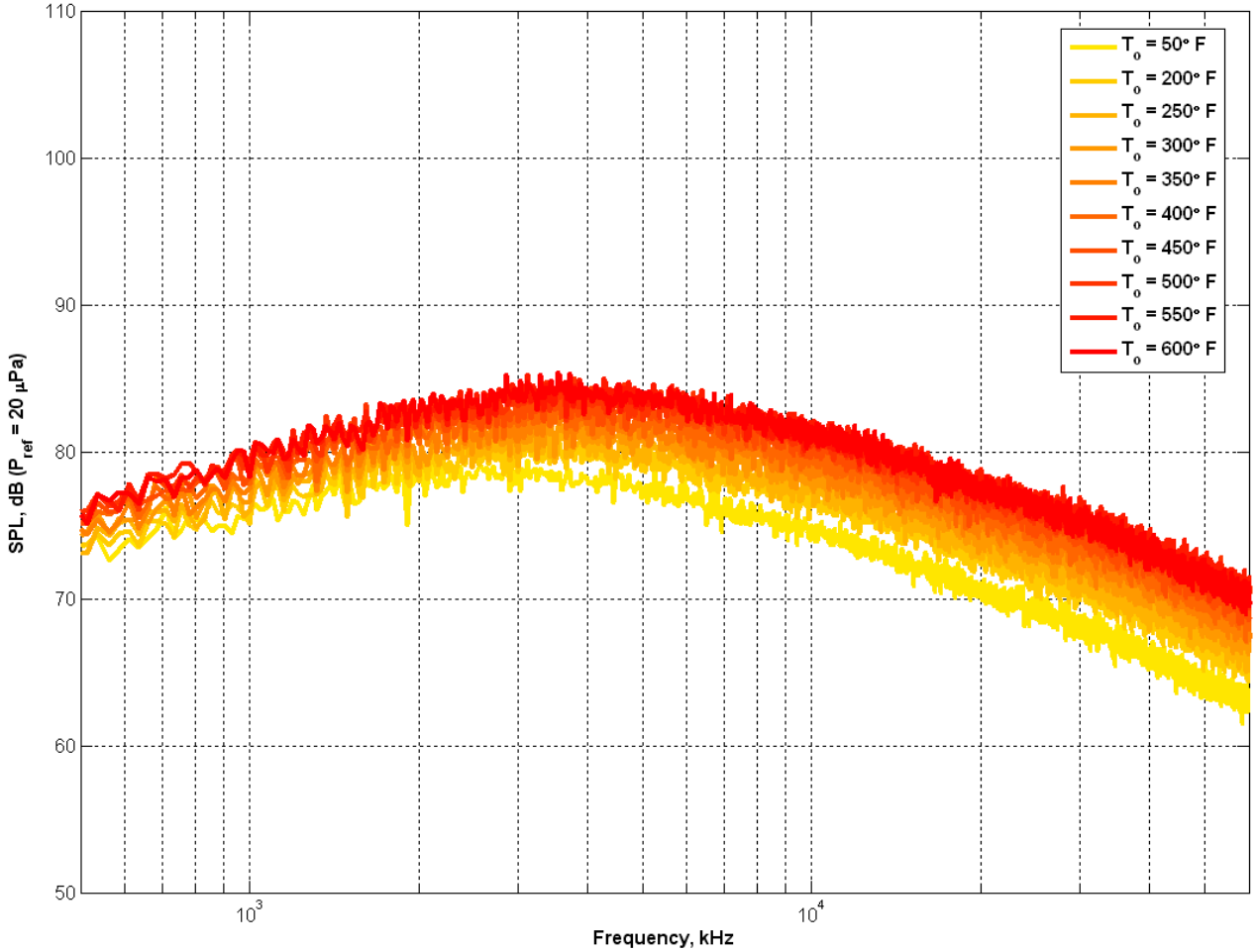

Figure 4.4 – Mach 0.9 heated jet spectra taken at $\theta = 90^0$. These are the raw data sets before any scaling has been applied.

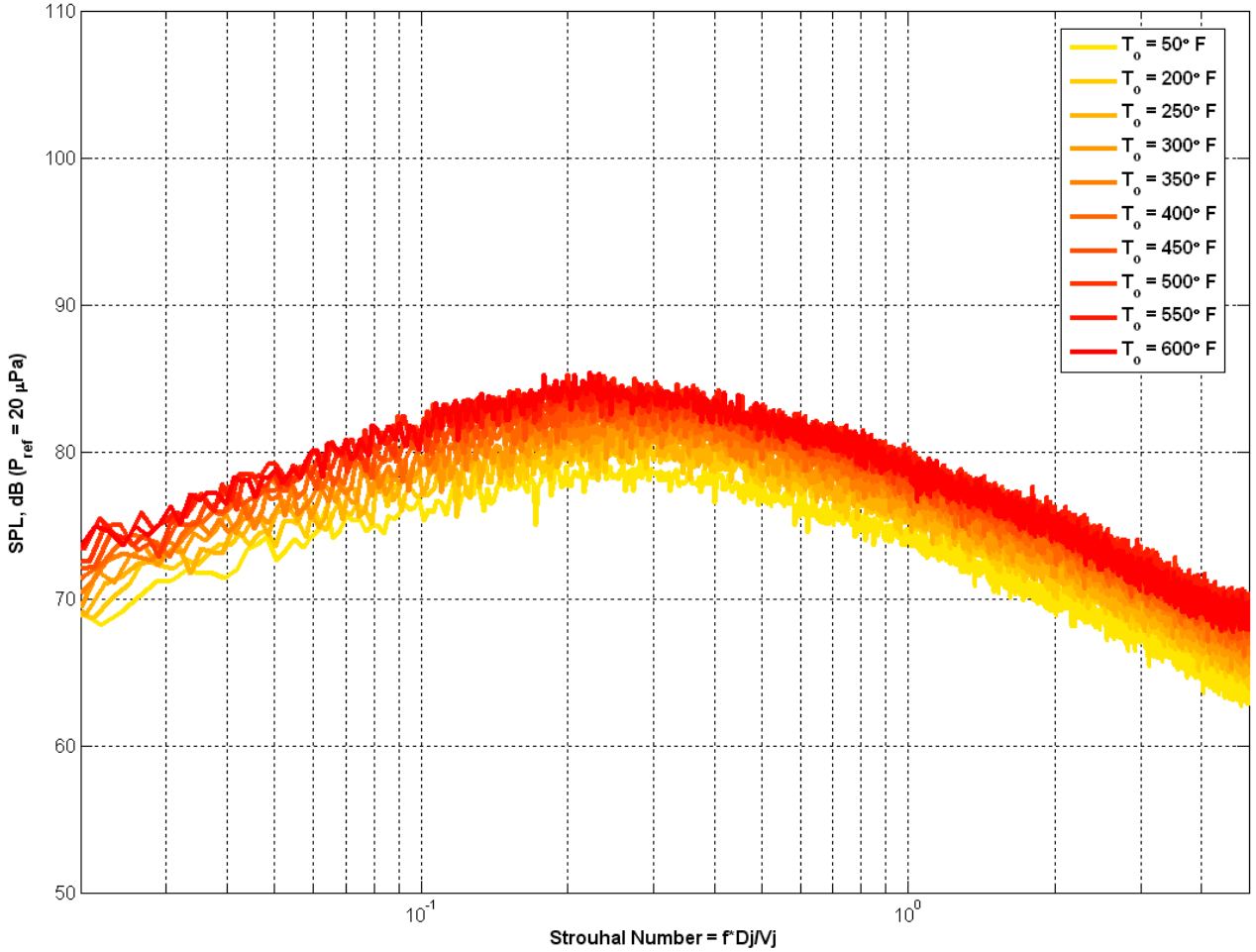

Figure 4.5 – Mach 0.9 heated jet spectra taken at $\theta = 90^0$. Frequency has been normalized by the Strouhal number.

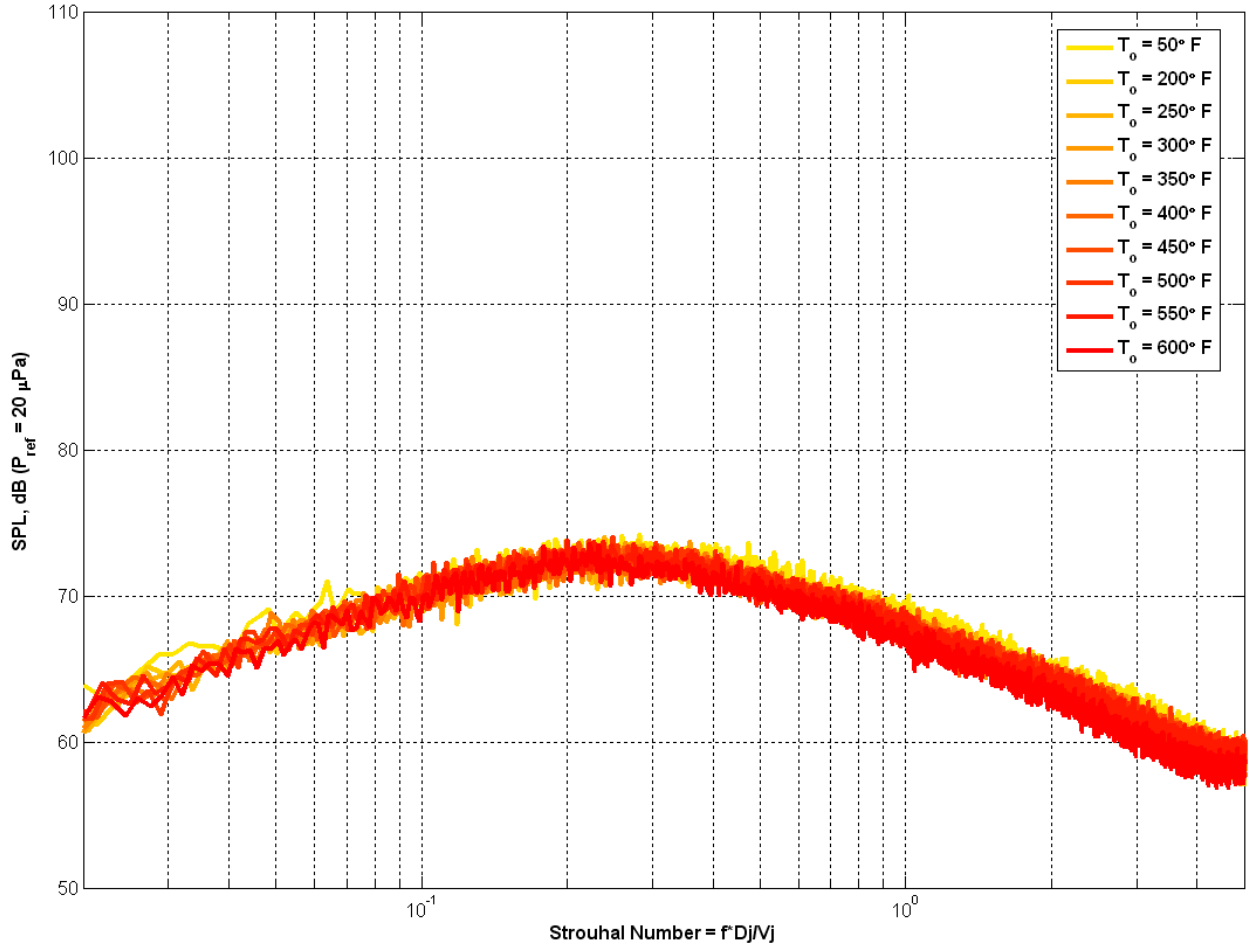

Figure 4.6 – Mach 0.9 heated jet spectra taken at $\theta = 90^0$. Frequency has been normalized by the Strouhal number and the SPL for each temperature has been normalized using equation (7).

4.2 – Discussion of Heated Jet Results – $\theta = 30^o$

Figure 4.1 shows the raw SPL spectrum plotted against frequency for each jet temperature at an observation angle of 30^o. As expected, increasing the jet temperature increases the overall peak noise level. This is because increasing the jet temperature increases the jet velocity as discussed in section 2.2 and since the noise is proportional to the jet velocity to a power, the noise increases with increasing temperature. Also in Figure 4.1, as the jet temperature increases, the frequency where the peak SPL occurs increases.

Figure 4.2 shows the same data set as in Figure 4.1 but with frequency normalized using the Strouhal number. After applying this normalization, all of the SPL peaks collapse onto a Strouhal number of around 0.18. This is a good sign since other 1 inch jets that have been used at the GDTL, including Mach 1.3 cold jets, all have their SPL peaks at this same Strouhal number (Hileman 2004, Southworth 2004) when observed from 30^o. This result helps to confirm that the Mach 0.9 nozzle is working properly and that no extraneous noise is present that may result in an SPL peak at a different Strouhal number and indicate contaminated flow.

Finally, Figure 4.3 shows the normalized SPL spectrum obtained using equation (6) vs. Strouhal number. All of the SPL peaks at each temperature now collapse onto the cold jet peak (50 ^{o}F) at a Strouhal number of around 0.18. The collapse of the SPL peaks at different temperatures onto the cold jet peak using equation (6) implies that the velocity increases associated with each increasing temperature are the main factors behind the overall noise increases seen in Figures 4.1 and 4.2. The good collapse of the data also implies that the jet noise data is clean and of high quality with no outside noise

affecting the recorded microphone signals such as unwanted noise from the storage heater.

One problem is noticeable from observation of Figure 4.3, though. This is the fact that for increasing temperature, the jet experiences a loss of SPL at higher frequencies above the peak SPL frequency. This is an effect that can potentially be attributed to a lowering of the jets Reynolds number with increasing temperature. Other researchers have shown a similar decrease in high frequency noise for lower Reynolds number jets (Viswanathan 2004, Kastner et. al 2005). It is likely that the jet boundary layer may be reverse-transitioning to laminar at the elevated temperatures.

Table 4.1 summarizes the effects of increasing jet temperature on the various jet parameters. As already discussed, increasing the jet temperature increases the jet speed of sound, which in turn increases the jet velocity for a constant Mach number. The significant lowering of the jet's Reynolds number with increasing temperature is also shown in Table 4.1.

To (^{o}F)	To (K)	T (K)	Jet Speed of Sound, a (m/s)	Uj (m/s)	ν (m^2/s)	Re
50	283	244	313	282	1.11E-05	6.47E+05
200	366	315	356	320	1.68E-05	4.84E+05
250	394	339	369	332	1.93E-05	4.37E+05
300	422	363	382	344	2.20E-05	3.97E+05
350	450	387	394	355	2.45E-05	3.68E+05
400	477	411	406	366	2.72E-05	3.41E+05
450	505	435	418	376	2.99E-05	3.20E+05
500	533	459	429	386	3.28E-05	2.99E+05
550	561	483	440	396	3.58E-05	2.81E+05
600	589	507	451	406	3.89E-05	2.65E+05
1000	811	698	529	477	6.59E-05	1.84E+05

Table 4.1 – The effect of temperature effects on the properties of the Mach 0.9 jet. 1000 ^{o}F was not run but is shown as an example since 1000 ^{o}F is the temperature that ideally needs to be reached.

4.3 – Discussion of Heated Jet Results – $\theta = 90^o$

The analysis carried out for the sound spectrums at 90^o is analogous to the analysis for the 30^o spectrums shown in section 4.2. Figure 4.4 shows the raw SPL data versus frequency obtained for the different jet temperatures at 90^o. Again, as the jet temperature increases, the jet velocity increases and so does the overall noise level. Also, as with 30^o, the peak frequency increases with increasing jet temperature. Figure 4.5 shows the same SPL spectrum data but with frequency again normalized by the Strouhal number. When normalized by Strouhal number, each different spectrum peak collapses onto a Strouhal number of around 0.23, which again is consistent with previous results at the GDTL for an observation angle of 90^o (Hileman 2004, Southworth 2004).

A closer look at Figure 4.4 shows that the peak SPL at 90^o does not increase as rapidly with increasing temperature as it does for the 30^o cases. To get a good collapse of the heated spectrums onto the cold jet spectrum for 90^o, as shown in Figure 4.6, required the velocity scaling to be done with an exponent of 4.2 as opposed to 8.0 for 30^o. This suggests that the radiated noise at 90^o is not as sensitive to jet velocity changes as the noise at 30^o. If Reynold's number effects are present in the flow, however, and the flow is becoming laminar, the boundary layer thickness at the jet nozzle exit will be decreased as temperature is increased. Since the boundary layer at the nozzle exit forms the initial shear layer of the jet, a decrease in the boundary layer thickness would greatly impact the noise spectrum at 90^o. It could be that a laminar jet flow is not as sensitive to velocity changes as a turbulent flow but more experiments would have to be run to test this possibility out.

4.4 – Exploring the Reynolds Number Effect and Boundary Tripping

From the heated jet spectra obtained at 30^{o}, it seems likely that the jet flow is reverse-transitioning to a laminar boundary layer and that this is causing a decrease in the SPL spectrums at higher frequencies. Since the overall goal of this research effort is to model the exhaust from a jet engine, the flow must be turbulent in order to provide an accurate model. If the flow is reverse-transitioning to laminar, different noise mechanisms may be becoming responsible for the noise generated and thus the jet model being used may not be accurate. Thus, turbulence is going to be added into the jet flow at the GDTL using a boundary layer tripping device.

As the final part of the research effort presented in this paper, a boundary tripping device has been designed and is shown in Figure 4.7. The device is actually fairly simple. The boundary trip extension, shown on the left in Figure 4.7, is a small cylinder that fits between the nozzle and the piping before the nozzle. The tripping device itself is a small ring, also shown on the left in Figure 4.7, that fits in between the nozzle and this new boundary trip extension. The inner surface of the ring is the same diameter as the jet flow passage before the nozzle and has been roughened up through machining. This rough surface will trip the jet flow as the flow passes over it before exiting the nozzle. Currently, two different rings with different roughness levels have been manufactured. More rings can be easily and inexpensively made since it is not yet known what level of roughness will be needed to add back in enough turbulence and it may require some amount of trial and error.

Figure 4.7 – (Left) The boundary trip extension and a trip ring. (Right) The boundary trip extension attached to the Mach 0.9 nozzle.

CHAPTER 5

SUMMARY AND RECOMMENDATIONS FOR FUTURE WORK

A new heated jet facility has recently been installed at the GDTL. This thesis has presented the first steps in using this new heated facility to determine the physical mechanisms of noise generation in a heated jet flow. First, the operation and trouble shooting of the storage heater used to provide heated flow was discussed in section 3.3. It was found that the heater did not perform to specifications and could only obtain an output temperature of 600 ^{o}F rather than the desired 1000 ^{o}F. The heater also took much longer than expected to provide the desired jet temperature. However, the heater did provide clean jet noise spectra and did not produce any extraneous noise that contaminated the microphone signals and jet noise results.

Since the heater could only reach a temperature of 600 ^{o}F, heated jet spectra were obtained from 50 ^{o}F to 600 ^{o}F at angles of 30^{o} and 90^{o} to the jet axis. Based on the theoretical background discussed in section 2.2, the jet noise was expected to increase with increasing temperature due to the fact that increasing the jet temperature increases the jet velocity and jet noise is proportional to the jet velocity to a power between 3 and 8. The SPL spectra obtained at 30^{o} and 90^{o} confirmed that the noise from the jet did increase as temperature was increased. Also, the jet spectra at different temperatures were scaled by jet velocity. The results show that each spectrum could be scaled well to the cold jet spectrum. This result helps show that the GDTL jet facility is operating well and that no outside noise contaminated any of the sound data. At 30^{o}, though, the jet

spectra experience a decrease in amplitude at higher frequencies, which seems to suggest that the flow may be reverse-transitioning to laminar as the jet temperature is increased and the jet's Reynolds number is lowered. Thus, a boundary-tripping device was designed to explore the effects of adding turbulence back into the flow and to help confirm the extent of the Reynolds number effects on the heated jet spectrums.

As for future work, at the time of writing this thesis the heater is being torn down and heavily modified in hopes of achieving a jet temperature of 1000 ^{o}F in a reasonable amount of heating time. One of the first steps to be taken with this research effort will be to confirm whether these new changes to the heater will finally enable it to perform to specifications and produce the jet temperatures necessary to accurately model jet engine exhaust flow. Once the heater is working properly, the boundary-tripping device can be tested with heated flow to determine the effects of boundary tripping and changes in the exit boundary layer characteristics on the jet SPL spectrum. If the boundary tripping device does indeed restore the necessary level of turbulence to the jet flow and the validity of the jet flow as a model for jet engine exhaust can be confirmed, heated jet flows of varying temperature can be studied and analyzed using the noise source localization techniques described in section 2.1 that were so successful for cold flow. It is hoped that this will lead to a new understanding of jet engine noise and reveal possible avenues for future noise control and reduction.

CHAPTER 6

RERFERENCES

Anderson, J. D., Modern Compressible Flow with Historical Perspective (3rd ed.). New York: McGraw-Hill Companies, 2003.

Antoine, N., "Aircraft Noise Overview," Stanford University, 2000.

Hileman, J., Caraballo, E., Thurow, B., and Samimy, M., "Differences in Dynamics of an Ideally Expanded Mach 1.3 Jet During Noise Generation and Relative Quiet Periods," AIAA Paper 2004-3015, May 2004.

Hileman, J., "Large-Scale Structures and Noise Generation in High-Speed Jets," Diss. The Ohio State University, 2004.

Hileman, J., Thurow, B., and Samimy, M., "Acoustic Source Localization Using a 3-D Microphone Array in a Mach 1.3 Jet," AIAA Paper 2002-0366, January 2002a.

Hileman, J., Thurow, B., and Samimy, M., "Exploring Noise Sources Using Simultaneous Acoustic Measurements and Real-time Flow Visualizations In Jets," *AIAA Journal*, Vol. 40, No. 12, December 2002b, pp. 2382-2392.

Kastner, J., Samimy, M., Hileman, J., Freund, J. B., "Comparison of Noise Sources in High and Low Reynolds Number High Speed Jets," AIAA Paper 2005-3092, May 2005.

Lighthill, M. J., "On Sound Generated Aerodynamically: I. General Theory," *Proc. Royal Soc. London*, Ser. A., Vol. 211, 1952, pp. 564-581.

Lighthill, M. J., "On Sound Generated Aerodynamically: II. Turbulence as a Source of Sound," *Proc. Royal Soc. London*, Ser. A., Vol. 222, 1954, pp. 1-32.

Lilley, G.M., (1991) "Jet Noise Classical Theory and Experiments," *Aeroacoustics of Flight Vehicles: Theory and Practice*. Vol. 1, ed. H.H. Hubbard, pp.211-290. NASA RP-1258.

Mani, R., "The Influence of Jet Flow on Jet Noise. Part 2. The Noise of Heated Jets," *Journal of Fluid Mechanics*, Vol. 73, Part 4, 1976, pp. 779-793.

Southworth, S., "Comparison of Radiation from Cold and Heated Jets," Undergraduate Thesis, The Ohio State University, 2004.

Tam, C.K.W., Golebiowski, M. and Seiner, J.M., "On the Two Components of Turbulent Mixing Noise from Supersonic Jets," AIAA paper 96-1716, Second Joint CEAS/AIAA Aeroacoustics Conference, State College, PA, 1996.

Viswanathan, K., "Aeroacoustics of Hot Jets," Journal of Fluid Mechanics Vol. 516, 2004, pg. 39-82.